Inorganic Chemistry

Article

pubs.acs.org/IC

Synthesis and SHG Properties of Two New Cyanurates: $Sr_3(O_3C_3N_3)_2$ (SCY) and $Eu_3(O_3C_3N_3)_2$ (ECY)

Markus Kalmutzki,[†] Markus Ströbele,[†] Frank Wackenhut,[‡] Alfred J. Meixner,[‡] and H.-Jürgen Meyer*[,†]

[†]Abteilung für Festkörperchemie und Theoretische Anorganische Chemie, Institut für Anorganische Chemie, Auf der Morgenstelle 18 Eberhard Karls Universität Tübingen, 72076 Tübingen, Germany

[‡]Institut für Physikalische und Theoretische Chemie Eberhard Karls, Universität Tübingen, Auf der Morgenstelle 18, 72076 Tübingen, Germany

Supporting Information

ABSTRACT: The new cyanurates $Sr_3(O_3C_3N_3)_2$ (SCY) and $Eu_3(O_3C_3N_3)_2$ (ECY) were prepared via exothermic solid state metathesis reactions from MCl_2 (M = Sr, Eu) and K(OCN) in silica tubes at 525 °C. Both structures were characterized by means of powder and single crystal X-ray diffraction, and their structures are shown to crystallize with the noncentrosymmetric space group *R*3*c* (No. 161). Infrared spectra and nonlinear optical properties (NLO) of SCY and ECY are reported in comparison to those of CCY and β-BaB_2O_4 (β-BBO).

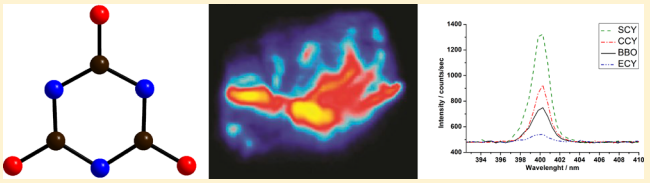

INTRODUCTION

A number of inorganic cyanurates are currently developed by us via solid state metathesis reactions, departing from a metal halide and alkali cyanate. Reactions like these have been investigated *in situ* by thermal analyses, revealing the reaction to occur at temperatures between 400 and 500 °C. It has also been shown that this type of reaction involves a local melt in which cyanate ions $(OCN)^-$ undergo a trimerization reaction to form the cyclic cyanurate ($(O_3C_3N_3)^{3-}$) ion.[1,2]

A growing number of examples have been developed following this relatively simple procedure: Reactions between Li(OCN) and $SrCl_2$ yielded $LiSr(O_3C_3N_3)_2$, and reactions between Li(OCN) and SrF_2 yielded $Li_3Sr_2F(O_3C_3N_3)_2$.[2] It turned out that a successful usage of Li(OCN) in these reactions is limited to its melting point (approximately 475 °C) because decomposition occurs right above this temperature.[3] A better performance has been obtained in reactions with K(OCN), which can be heated up to at least 550 °C without decomposition.[1] Moreover, we have developed rare earth (REs) compounds with the general formula $ARE_2Cl(O_3C_3N_3)_2$ from reactions of A(OCN) (A = K, Rb, Cs) and $RECl_3$ (RE = La, Ce, Pr). Photoluminescence properties of $ALa_2Cl(O_3C_3N_3)_2$ with A = K and Rb have been reported for Tb^{3+}- and Eu^{3+}-doped samples.[4]

The first binary cyanurate was recently reported as $Ba_3(O_3C_3N_3)_2$ (BCY), prepared from a mixture of $BaCl_2$ and K(OCN). The crystal structure of BCY has been shown to crystallize in the centrosymmetric space group $R\bar{3}c$, isotypic to the high temperature modification of BaB_2O_4 (α-BBO), whose structure contains cyclic $(B_3O_6)^{3-}$ ions.[1] Afterward we succeeded in synthesizing $Ca_3(O_3C_3N_3)_2$ (CCY) which crystallizes with the noncentrosymmetric space group *R*3*c*, isotypic to the low temperature modification of BaB_2O_4 (β-BBO), which is considered one of the most important nonlinear optical (NLO) materials.[5] NLO materials with frequency doubling (second harmonic generation, SHG) properties are important materials in several optical applications such as the generation of laser beams in the visual region, laser medicine, optical data transmission and processing, and optical data storage.

Very recently NLO measurements on crystalline samples have shown CCY to have an NLO efficiency one magnitude larger than β-BBO.[5] Here we present the syntheses and structures of $Sr_3(O_3C_3N_3)_2$ (SCO) and $Eu_3(O_3C_3N_3)_2$ (ECO) together with their NLO properties, in comparison to results on the aforementioned NLO materials.

EXPERIMENTAL SECTION

Preparation. Manipulations of starting materials were performed in a glovebox under dry argon atmosphere. The preparation of K(OCN) was previously described.[1] $SrCl_2$ (99.5%, Alfa Aesar) and $EuCl_2$ (99.99%, Aldrich) were used as purchased without any further purification. $M_3(O_3C_3N_3)_2$ was prepared from a mixture of MCl_2 (M = Sr, Eu) and K(OCN) with 1:2 molar ratio following eq 1.

$$3MCl_2 + 6K(OCN) \rightarrow M_3(O_3C_3N_3)_2 + 6KCl \quad (1)$$

The mixtures were carefully ground in an agate mortar, loaded into silica ampules, and fused therein under vacuum. Reactions were performed in a chamber furnace by heating the ampules to 525 °C within 4 h, with a holding time of 6 h at this temperature, before cooling down with the natural cooling rate of the furnace. Ampules were opened in air and rinsed several times, first with water and afterward with dry ethanol. The crystalline product was inspected by powder X-ray diffraction (XRD). XRD powder patterns indicate quantitative conversion rates of reactions, by showing only reflections of the product and the metathesis salt (KCl). Single crystals were selected for crystal structure XRD determination.

Received: September 1, 2014
Published: November 7, 2014

β-BaB_2O_4 (β-BBO) was synthesized by reacting $BaCO_3$ and H_2BO_3 in a 1:1 ratio. The reactants were mixed in an agate mortar and heated up to 800 °C in a corundum vessel remaining at this temperature for 4 h before cooling down with the natural cooling rate of the furnace.[6]

X-ray Diffraction. Powder XRD patterns were collected with a Stadi-P (STOE, Darmstadt) diffractometer using germanium monochromated Cu $K_{\alpha 1}$ radiation. Single crystals of $M_3(O_3C_3N_3)_2$ (M = Sr, Eu) were measured with a single crystal X-ray diffractometer (STOE-IPDS) by using Mo Kα radiation (λ = 0.710 73 Å) at room temperature. Crystal structure solutions were attempted with direct methods (SHELXS), and refinements were performed with SHELXL including least-squares refinements on F^2.[7]

The crystal structure of $Sr_3(O_3C_3N_3)_2$ (SCY) was refined on a transparent single crystal (ca. 0.10 × 0.04 × 0.03 mm^3) within the range Θ = 3.44−24.71. A total number of 4659 collected reflections was corrected for Lorentz and polarization effects (STOE IPDS Software) and reduced to 590 independent reflections (R_{int} = 0.0872).

The structure of $Eu_3(O_3C_3N_3)_2$ (ECY) was refined on a transparent yellow single-crystal (ca. 0.11 × 0.05 × 0.03 mm^3) within the range Θ = 3.80−25.95. A total number of 4415 collected reflections was corrected for Lorentz and polarization effects (STOE IPDS Software) and reduced to 667 independent reflections (R_{int} = 0.0788).

Some results and final R values for the structure of SCY and ECY are shown in Table 1; atom positions and isotopic displacement parameters are collected in Table 2 (SCY) and Table 3 (ECY). Selected bond length and angles of CCY, SCY, and ECY are compared in Table 4.

Table 1. Crystal Data and Structure Refinement Parameters of SCY and ECY

	$Sr_3(O_3C_3N_3)_2$	$Eu_3(O_3C_3N_3)_2$
fw (g/mol)	514.98	708.00
syst, space group, Z	trigonal, *R3c* (No. 161), 6	trigonal, *R3c* (No. 161), 6
unit cell dimensions (Å)	a = 11.8620(2)	a = 11.8570(2)
	c = 12.6983(3)	c = 12.5640(3)
unit cell volume ($Å^3$)	1547.36(5)	1529.71(5)
d_{calc} (mg/m^3)	3.316	4.611
μ (mm^{-1}) (Mo Kα)	15.503	18.271
R1, wR2 (all data)	0.0307, 0.0707	0.0379, 0.0842

Table 2. Atom Positions and Isotropic Displacement Parameters ($pm^2 \times 10^{-1}$) of SCY

atom	x	y	z	U_{eq}[a]
Sr(1)	0.6714(1)	0.9815(1)	0.9539(1)	40(1)
C(1)	0.6428(8)	0.2124(8)	0.0955(6)	37(2)
N(1)	0.7113(7)	0.4636(6)	0.8389(5)	43(2)
O(1)	0.5795(5)	0.0838(5)	0.8306(5)	53(1)
C(2)	0.6228(8)	0.2075(8)	0.8357(5)	38(2)
N(2)	0.7686(7)	0.3101(7)	0.0954(5)	41(2)
O(2)	0.9073(5)	0.5257(5)	0.1000(4)	46(1)

[a] U_{eq} is defined as one-third of the trace of the orthogonalized U_{ij} tensor. All atoms occupy 18b sites.

Thermal Analysis. Differential scanning calorimetry (DSC) measurements were performed in a Netzsch Jupiter, STA 449 F3 apparatus. A sample of about 30 mg SCY was enclosed into a gold plated stainless steel capsule and heated in a cyclic procedure between room temperature and 700 °C.

Infrared Spectroscopy. Vibrational spectra were recorded on a Bruker Tensor 27 FT-IR spectrometer within the range 400−4000 cm^{-1} by using KBr pellets.

Reflection Spectroscopy. Reflection spectra were recorded on an Edinburgh Instruments FS900 spectrometer equipped with a 450 W Xe arc lamp and cooled single-photon counting photomultiplier (Hamamatsu R928). $BaSO_4$ (99%, Sigma-Aldrich) was used as a reflectance standard.

Table 3. Atom Positions and Isotropic Displacement Parameters ($pm^2 \times 10^{-1}$) of ECY

atom	x	y	z	U_{eq}[a]
Eu(1)	0.6707(1)	0.9811(1)	0.9544(1)	37(1)
C(1)	0.6404(14)	0.2109(12)	0.0935(13)	33(3)
N(1)	0.7078(12)	0.4630(12)	0.8333(11)	42(3)
O(1)	0.5822(11)	0.0844(10)	0.8277(11)	55(3)
C(2)	0.6250(14)	0.2073(14)	0.8332(12)	36(3)
N(2)	0.7681(13)	0.3072(12)	0.0945(12)	40(3)
O(2)	0.9066(9)	0.5260(10)	0.1010(9)	45(2)

[a] U_{eq} is defined as one-third of the trace of the orthogonalized U_{ij} tensor. All atoms occupy 18b sites.

Table 4. Comparison of Selected Angles (in deg) in Cyanurate Ions of Isotypic MCY compounds with M = Calcium, Strontium, and Europium

angle	CCY	SCY	ECY
[C(1)−N(2)−C(1)]	115.9(3)	116.2(8)	115.6(14)
[C(2)−N(1)−C(2)]	117.3(3)	116.4(8)	116.9(14)
[O(1)−C(2)−N(1)]	117.1(3)	118.0(8)	116.8(14)
	120.2(3)	118.6(7)	120.0(13)
[O(2)−C(1)−N(2)]	116.1(3)	117.3(8)	115.9(12)
	119.8(3)	118.8(7)	119.5(13)
[N(1)−C(2)−N(1)]	122.7(3)	123.5(8)	123.1(14)
[N(2)−C(1)−N(2)]	124.1(3)	123.8(8)	124.4(14)

NLO Measurements. All non-linear optical measurements were performed on a home-built inverted confocal microscope, which is equipped with a pulsed laser for excitation (Coherent RegA 9000; wavelength, 800 nm; pulse duration, 150 fs; repetition rate, 250 kHz). A scanning table was used to raster scan the specimen through the diffraction limited focus of an immersion oil objective lens with a numerical aperture of 1.25. The detected signal was collected with the same objective and guided to an avalanche photodiode for imaging or to a spectroscopic unit to acquire the nonlinear spectra. Further details about the experimental setup have been previously reported.[8]

RESULTS AND DISCUSSION

Crystal Structure. The crystal structures of the alkaline earth cyanurates SCY and ECY are isotypic to that of CCY, crystallizing with the noncentrosymmetric space group *R3c* (Table 1).[5] The same structure has been previously reported for β-BBO which is an important NLO material. The crystal structures of SCY and ECY contain two crystallographically distinct cyanurate rings (Tables 2 and 3) containing the cyclic $[C_3N_3]$ moiety with three exocyclic oxygen atoms forming the planar $(O_3C_3N_3)^{3-}$ ion. The distances and angles within cyanurate ions of the three compounds CCY, SCY, and ECY deviate insignificantly to each other (Table 4), most likely due to different ionic cationic radii and resulting matrix effects in structures.

The $(O_3C_3N_3)^{3-}$ ion is isoelectronic and isostructural to the $(B_3O_6)^{3-}$ ion in β-BBO. As can be predicted, the interatomic distances in the cyanurate rings of SCY and ECY are shorter than those found in the oxoborate ions $(B_3O_6)^{3-}$ in BBO (Figure 1).

The smaller cyanurate ring combined with the smaller Sr^{2+} and Eu^{2+} ions, compared to Ba^{2+} in BBO, make it reasonable that SCY and ECY adopt the same structure as β-BBO. BCY, with the larger Ba^{2+} ion, adopts the same crystal structure as the

dx.doi.org/10.1021/ic502035b | Inorg. Chem. 2014, 53, 12540−12545

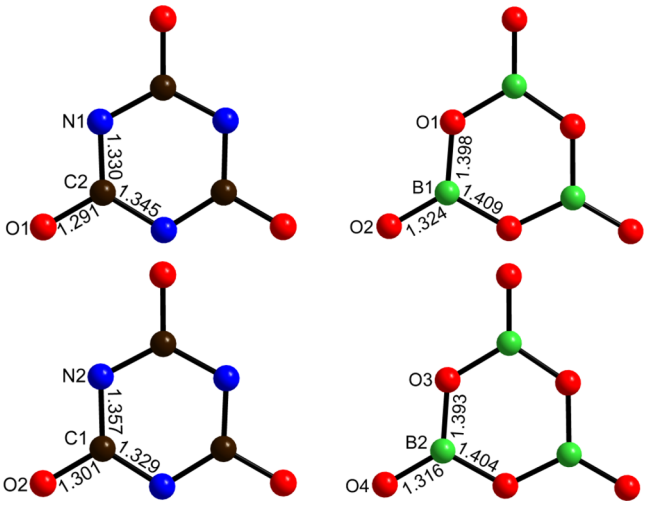

Figure 1. Comparison of $(O_3C_3N_3)^{3-}$ in SCY (left) and $(B_3O_3O_3)^{3-}$ ions in β-BBO (right).

high temperature modification α-BBO. Ongoing studies on SCY have revealed its dimorphic nature, with the existence of a high temperature modification under certain conditions.

This reveals a trend for cyanurate compounds, showing that the noncentrosymmetric LT-phase is formed by smaller cations (Ca, Eu, Sr), whereas the centrosymmetric HT phase is accessible by using larger cations (Sr, Ba). An analogous trend cannot be observed for the isotypic borate compounds. BBO crystallizes in both modifications whereas strontium borate (SrB_2O_4) appears with a different crystal structure containing BO_3 instead of B_3O_6 units.[6,9]

The crystal structures of SCY and ECY contain two crystallographically distinct cyanurate ions stacked on top of each other to form columns following the motif of hexagonal closest stick-packing, shown in Figure 2.

The cyanurate rings in columns (Figure 2) are contorted relative to each other around the 3-fold axis by approximately 10°/19.4° (SCY) and 11°/19.1° (ECY). A similar torsion can be found for borate rings in the crystal structure of β-BBO (approximately 9° and 20°).

The $(O_3C_3N_3)^{3-}$ ions are situated perpendicular to the polar 3-fold axis with their ring planes to form columns parallel to the c-axis, and layers along the ab-plane. Adjacent $(O_3C_3N_3)^{3-}$ ions exhibit alternating distances along their stacking direction (c-axis) which are 302.3 and 332.6 pm for SCY, and 295.3 and 332.9 pm for ECY. All these distances are shorter than interlayer distances in the structures of graphite (335 pm) and BN (333 pm).

The cations in MCY comprise one crystallographic position each, being situated in-between cyanurate layers and between the closest stick packing made up by cyanurate columns. It is interesting to note that the rotations of cyanurate rings also affect the positions and coordination environments of cations, having distorted trigonal prismatic environments formed by six oxygen atoms of six surrounding cyanurate ions, as shown in Figure 3. The M−O distances are at 253.3(5)−309.7(7) pm for

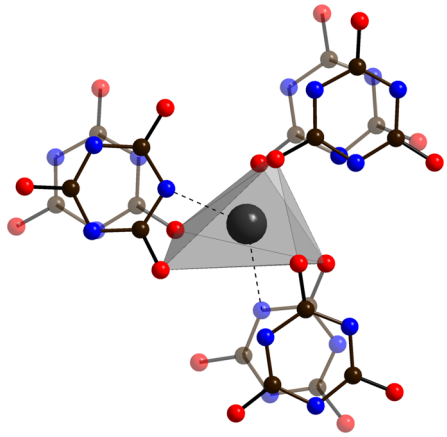

Figure 3. Distorted trigonal prismatic coordination environment of Sr^{2+} ions in crystal structure of SCY.

SCY, and at 253.4(12)−302.3(14) pm for ECY. In additon there are two short M−N contacts at 257.4(12)−260.5(7) pm due to the rigid nature of the cyanurate ions.

A comparison of interatomic distances and angles of the $(O_3C_3N_3)^{3-}$ ions found in SCY and ECY with those described for solid cyanuric acid[10] shows that a structural change takes place due to ionization. The average C−O bond length (121.45 pm) in solid cyanuric acid is close to the value expected for a C−O double bond (122 pm). The average C−O bond length

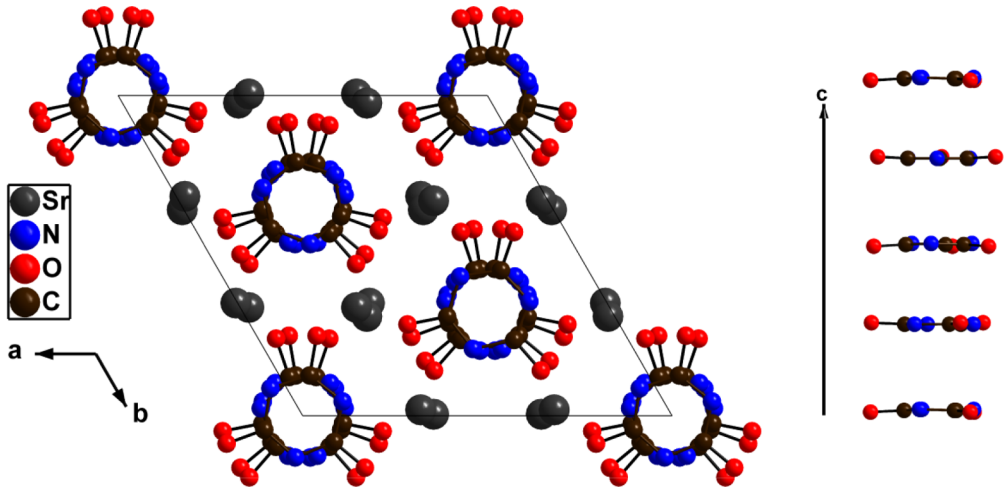

Figure 2. Projection of the crystal structure of SCY along the c-axis.

dx.doi.org/10.1021/ic502035b | Inorg. Chem. 2014, 53, 12540−12545

in SCY (129.6 pm) and ECY (128.7 pm) appears quite longer than a typical C−O double bond. Both SCY and ECY show alternating C−N distances in the $[C_3N_3]$-units with average C−N bond lengths of 134.0 pm (SCY) and 134.7 pm (ECY) that are found to be slightly shorter than in cyanuric acid (136.68 pm). From these findings it can be assumed that the negative charge of the cyanurate ion cannot be addressed to one type of atom in the cyanurate but is more likely to be delocalized on the whole molecule.

The average angles between three adjacent atoms in the cyanurate ion of 117.52° (SCY) and 117.43° (ECY) are close to theoretically expected angle of 120° as well as to the angle found in cyanuric acid (122.42°). All observed interatomic distances are close to theoretical values.[11]

Thermal Analysis. The thermal stability and melting behavior of SCY were investigated by DSC measurements. For this purpose a pure sample of SCY (dried under vacuum at 200 °C for 2 h) was examined in the temperature regime between room temperature and 700 °C in a cyclic procedure. Figure 4 shows congruent melting of SCY with onset points at

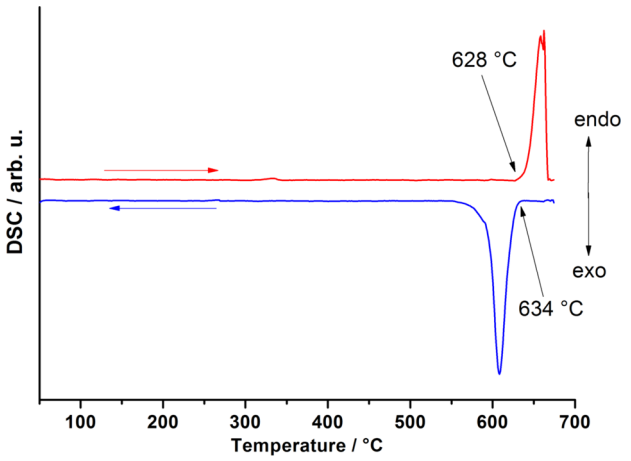

Figure 4. DSC measurement of SCY showing congruent melting and recrystallization.

628 °C for melting and 634 °C for recrystallization. The identity and purity of the sample after the DSC treatment was confirmed by powder XRD measurements.

Reflection Spectroscopy. The reflection spectrum of SCY is displayed in Figure 5. The spectrum shows a distinct absorption edge at about 420 nm (2.95 eV), which can interpreted to represent the position of the band gap. According to the electronic structure of a D_{3h} idealized cyanurate ion, a set of two degenerate π levels form the highest occupied energy levels (HOMO).[1] Corresponding anionic states of borate ions represent the valence band of β-BBO and a mixture mainly of boron (p) and barium (d) states represent the bottom of the conduction band, which leads to an expected band gap (theoretically and experimentally by XPS) on the order of 6 eV.[1213]

The smaller band gap obtained for SCY can be understood by comparing the UV−vis spectra of $(B_3O_6)^{3-}$ and cyanuric acid. The $\pi-\pi^*$ transition for $(B_3O_6)^{3-}$ in β-BBO was reported at 185 nm; the corresponding transition for cyanuric acid is located below 230−240 nm.[14,15]

Infrared Spectroscopy. Infrared spectra of $M_3(O_3C_3N_3)_2$ (M = Sr, Eu) were recorded between 2000 and 400 cm^{-1}. The spectra of our cyanurate compounds show characteristic

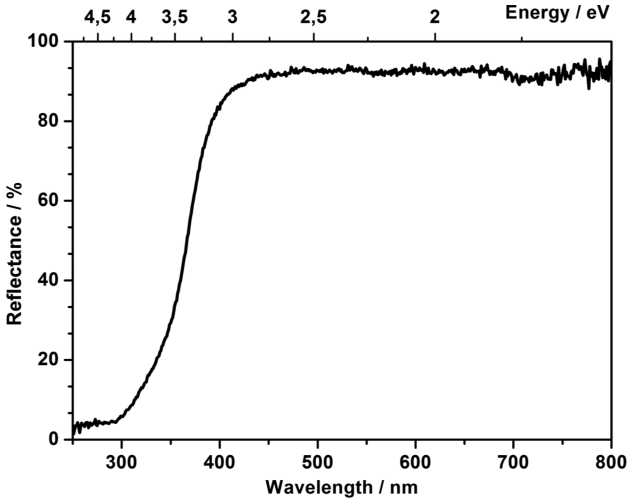

Figure 5. Reflection spectrum of SCY between 250 and 800 nm.

absorptions in the region 1500−1130 cm^{-1} for SCY and 1515−1140 cm^{-1} for ECY which correspond to stretching vibrations $\nu(C_3N_3)$. In-plane bending vibrations $\delta_{ip}(C_3N_3)$ are found at 618 cm^{-1} for SCY and at 624 cm^{-1} for ECY; out-of-plane bending vibrations $\delta_{oop}(C_3N_3)$ are found at 825 cm^{-1} for SCY and at 830 cm^{-1} for ECY.[1,16] Vibration bands belonging to cyanate were not obtained as expected for a single-phase products.

NLO Measurements. Second harmonic generation (SHG) is a second order nonlinear optical process in which two photons interact with a nonlinear material and one photon with doubled energy is created. This effect was first observed by Franken et al.[17] and is based on the interaction of light with the nonlinear terms of the materials polarization, which can be written as

$$P = \varepsilon_0(\chi E + \chi_2 E^2 + \chi_3 E^3 + ...) \quad (2)$$

with P, polarization; ε_0, free space electric permittivity; χ, linear susceptibility; $\chi_{2,3}$, nonlinear susceptibility terms; E, electric field.

Usually the linear susceptibility χ is much larger compared to the nonlinear terms $\chi_{2,3}$. However, for intense electric fields E, e.g., in the focus of a short laser pulse, and materials with high values for $\chi_{2,3}$, these nonlinear terms of the polarization can have a significant contribution. A well-known example for a material with high nonlinear susceptibility is β-BBO, which will serve as a reference material in this work.[6,18]

The structure of β-BBO features planar (B_3O_6) groups as its main building unit. The contribution of the localized π-conjugate orbital system on these (B_3O_6) units is considered to be the main reason for high SHG coefficients and thus high SHG efficiency of β-BBO, whereas the contribution of Ba^{2+} ions to the macroscopic SHG coefficients is negligible.[15,19,20] Since $(B_3O_6)^{3-}$ and $(O_3C_3N_3)^{3-}$ ions are isostructural, it can be assumed that both β-BBO and the isotypic cyanurate compounds show resembling nonlinear susceptibilities.

The optical measurements presented in this work were performed on a home-built confocal microscope described in the Experimental Section. In Figure 6 scan images of the nonlinear signal intensity produced by crystals consisting of β-BBO (a), SCY (b), CCY (c), and ECY (d) are shown.

All images in Figure 6 are recorded with an excitation power of 100 μW and are scaled to the maximum nonlinear signal

dx.doi.org/10.1021/ic502035b | Inorg. Chem. 2014, 53, 12540−12545

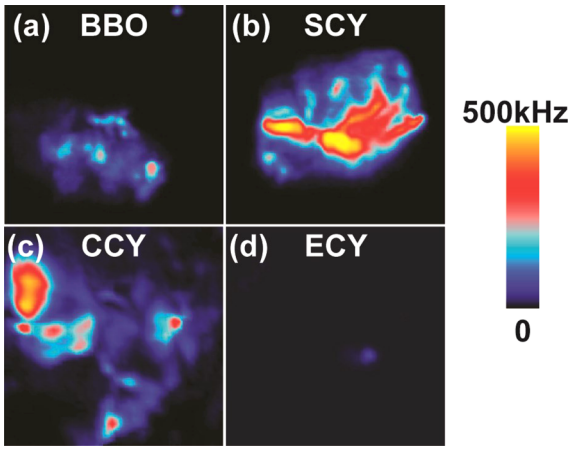

Figure 6. Scan images of the nonlinear signal intensity of crystals composed of β-BBO (a), SCY (b), CCY (c), and ECY (d). In general all materials exhibit an inhomogeneous distribution of the nonlinear signal intensity with the highest nonlinear signal intensity being observed for SCY (b), while hardly any nonlinear signal was detected for ECY (d). All images are scaled to the maximum intensity observed for SCY (b); the scan area is 15 × 15 μm^2 for all images.

intensity observed for SCY. The images of crystals composed of CCY and SCY are shown in Figure 6b,c. The nonlinear signal intensity exceeds the one observed for β-BBO (a) for both materials. For ECY only a weak nonlinear signal can be detected as shown in the nonlinear scan image of an ECY crystal in Figure 6d. In general all materials exhibit a similar inhomogeneous distribution of the nonlinear signal intensity, and only weak nonlinear signal intensities can be observed for most regions of the crystals. Nevertheless, there are hot spots with significantly increased nonlinear signal intensity which were utilized for the spectral characterization shown in Figure 7.

In Figure 7a, the nonlinear spectra of β-BBO (black line), SCY (green dashed line), CCY (red dotted line), and ECY (blue dash dotted line) under excitation at 800 nm with an excitation power of 20 μW are shown. The only spectral feature is the SHG signal at 400 nm which is clearly visible, even for such a low excitation power. Another spectral feature, which is common to all four materials, is that no two-photon luminescence is detectable for this excitation wavelength, and the only observed nonlinear signal is SHG. Figure 7b shows the spectral region around the SHG peak for the four different materials in more detail. The detected SHG intensity of SCY and CCY does again exceed that of β-BBO. ECY exhibits the weakest SHG intensity of all four materials. This is most likely due to the orange bodycolor leading to reabsorption effects. Figure 7c displays the excitation power dependence of the SHG signal intensity in a double logarithmic representation. The signal intensity is, as can be seen in eq 2 for a second order nonlinear process (like SHG), proportional to the square of the excitation power, which results in a slope of the linear fits of approximately 2 (2.06 for β-BBO, 1.94 for SCY, 2.07 for CCY, and 1.96 for ECY) as depicted in Figure 7c. This clearly proves that the observed signal is a two photon process, and together with the peak position, we can conclude that its origin is indeed SHG. Figure 7c clearly shows that the SHG efficiency of SCY and CCY significantly exceeds the efficiency of β-BBO, while ECY again exhibits a comparably weak SHG intensity. The high efficiency together with the absence of two-photon luminescence makes SCY a promising candidate to replace β-BBO for applications, e.g., frequency doubling of lasers.

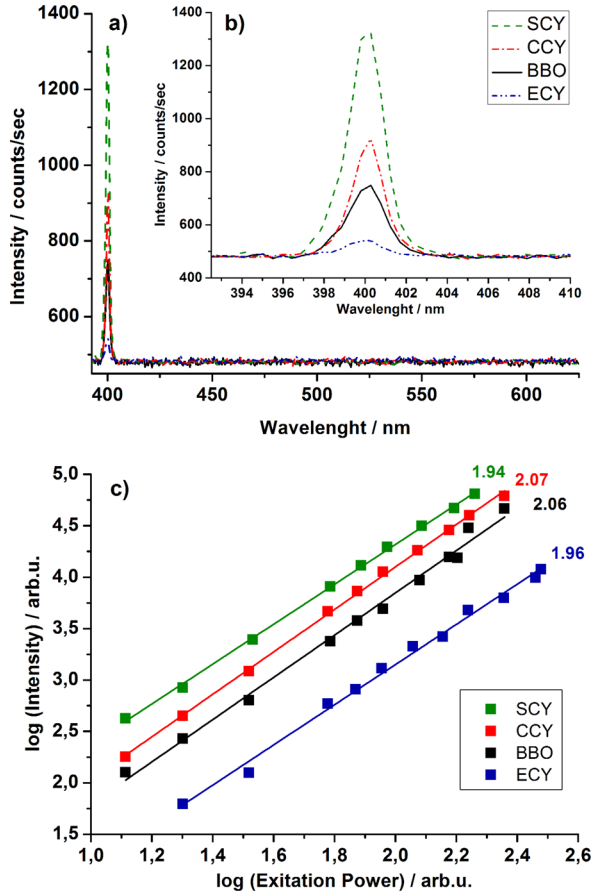

Figure 7. Nonlinear optical spectra of β-BBO (black line), SCY (green dashed line), CCY (red dotted line), and ECY (blue dash dotted line) are shown in (a) for an excitation power of 20 μW. In this spectral region no two-photon luminescence can be observed, and the only detectable signal is the SHG peak at 400 nm. (b) Spectral region around the SHG peak. In part (c), the excitation power dependence of the SHG signal of β-BBO (black), SCY (green), CCY (red), and ECY (blue) is shown in a double logarithmic representation. The continuous lines are corresponding linear fits, and their slopes are for all four materials close to 2. One can clearly see that for the investigated range of excitation power CCY and SCY do exhibit a more efficient SHG than β-BBO.

■ ASSOCIATED CONTENT

Ⓢ Supporting Information

CIF data for $Sr_3(O_3C_3N_3)_2$ and $Eu_3(O_3C_3N_3)_2$. This material is available free of charge via the Internet at http://pubs.acs.org.

■ AUTHOR INFORMATION

Corresponding Author

*E-mail: juergen.meyer@uni-tuebingen.de. Fax: (+49)7071-29-5702.

Notes

The authors declare no competing financial interest.

■ ACKNOWLEDGMENTS

Support of this work by the Deutsche Forschungsgemeinschaft (Bonn) through Grant ME914/25-1 is gratefully acknowledged. M.K. is indebted to the Landesgraduiertenförderung of

the Science Ministry of Baden-Württemberg as well as the Institutional Strategy of the University of Tübingen (Deutsche Forschungsgemeinschaft, ZUK 63). The authors would like to thank Prof. Dr. T. Jüstel and M.Sc. David Enseling for the measurement of refection spectra.

REFERENCES

(1) Kalmutzki, M.; Ströbele, M.; Bettinger, H. F.; Meyer, H.-J. *Eur. J. Inorg. Chem.* **2014**, 2536−2543.
(2) Kalmutzki, M.; Ströbele, M.; Meyer, H.-J. *Dalton Trans.* **2013**, *42*, 12934−12939.
(3) Hennings, E.; Schmidt, H.; Voigt, W. *Z. Anorg. Allg. Chem.* **2011**, *637*, 1199−1202.
(4) Kalmutzki, M.; Ströbele, M.; Enseling, D.; Jüstel, T.; Meyer, H.-J. *Eur. J. Inorg. Chem.* **2014**, accepted.
(5) Kalmutzki, M.; Ströbele, M.; Wackenhut, F.; Meixner, A.; Meyer, H.-J. *Angew. Chem.* **2014**, in press.
(6) Liu, J.; Wang, X.-D.; Wu, Z.-C.; Kuang, S.-P. *Spectrochim. Acta, Part A* **2011**, *79*, 1520−1523.
(7) Sheldrick, G. M. *Acta Crystallogr.* **2008**, *A64*, 112.
(8) (a) Wackenhut, F.; Failla, A. V.; Züchner, T.; Steiner, M.; Meixner, A. J. *Appl. Phys. Lett.* **2012**, *100*, 263102−263104. (b) Wackenhut, F.; Failla, A. V.; Meixner, A. J. *J. Phys. Chem. C* **2013**, *117*, 17870−17877.
(9) Zhao, L.-S; Liu, J.; Wu, Z.-C.; Kuang, S.-P. *Spectrochim. Acta, Part A* **2012**, *87*, 228−231.
(10) Chen, C.-Z.; Shi, J.-Q.; Lin, Z.-B.; Gao, D.-S.; Huang, X.-Y.; Li, D. *Jiegou Huaxue* **1995**, *14*, 241−244.
(11) Shannon, R. D. *Acta Crystallogr., Sect. A* **1976**, *A32*, 751−767.
(12) Cheng, W.-D.; Huang, J.-S.; Lu, J.-X. *Phys. Rev. B* **1998**, *57*, 1527−1533.
(13) Xu, Y.-N.; Ching, W. Y.; French, R. H. *Phys. Rev. B* **1993**, *48*, 17695−17702.
(14) Klotz, I. M.; Askounts, T. *J. Am. Chem. Soc.* **1947**, *69*, 801−803.
(15) Che, C.; Sasaki, T.; et al. *Nonlinear Optical Borate Crystals: Principles and Applications*; Wiley VCH: New York, 2012.
(16) Hesse, M.; Meier, H.; Zeeh, B. *Spektroskopische Methoden in der Organischen Chemie*; Georg Thieme Verlag: Stuttgart, 2005.
(17) Franken, P. A.; Hill, A. E.; Peters, C. W.; Weinreich, G. *Phys. Rev. Lett.* **1961**, *7*, 118−119.
(18) Nikogosyan, D. N. *Appl. Phys. A: Mater. Sci. Process.* **1991**, *52*, 359−368.
(19) Byrappa, K.; Ohachi, T. *Crystal Growth Technology*; Springer: New York, 2003.
(20) Lin, Z. S.; Lin, J.; Wang, Z. Z.; Wu, Y. C.; Ye, N.; Chen, C. T.; Li, R. K. *J. Phys.: Condens. Matter* **2001**, *13*, 369−384.